A Capillary-Fed Annular Colloid Thruster

ADRIAN G. BAILEY,* JÖRG E. BRACHER,† AND HANS J. VON ROHDEN‡
European Space Research and Technology Centre, Noordwijk aan Zee, The Netherlands

The operating characteristics of a capillary-fed annular colloid thruster are presented. There is little difference in thruster performance between positive and negative thruster operation. The experimental thruster voltage/current characteristic resembles a zener diode characteristic in that the thruster voltage only changes by 15% over a current range of 50–400 μa. Over this operating range, the propellant mass-flow rate is practically constant. With this assumption, together with the assumption that thruster voltage is also constant over the operating range, it is shown that thrust and exhaust velocity are linear functions of the square root of operating current. It follows that a maximum thruster efficiency is approached at the highest current operating levels.

Introduction

EXPERIMENTAL studies of both linear and annular-slit colloid thrusters have been undertaken at the European Space Research and Technology Centre (ESTEC), in the Netherlands, during the last three years. Direct thrust and mass-flow rate measurements have been made by means of a horizontal torsion balance which is described elsewhere.[1] Initial feasibility studies were confined to colloid thrusters of the linear-slit type. A 2-cm-long linear thruster made from standard razor blades had the following performance data: thrust $= 10^{-4}$N, mean exhaust velocity $= 12$ km/sec, over-all efficiency $= 50\%$.

Because of certain manufacturing problems, it was decided, having demonstrated the feasibility of colloid thrusters, to concentrate on the annular configuration. The results of this annular thruster study are presented here.

Because the complexity of the relationships[2] between the usual thruster control variables such as mass-flow rate of propellant ($\dot{m}$), acceleration voltage (V), emitter geometry, emitter temperature and propellant properties, it was decided to reduce several of these parameters to constant values. Of particular importance, was the decision to feed the thruster by capillary forces alone (no pressure feeding) in the hope that $\dot{m}$ would not change very much over the thruster operating range. This hope was, in fact, borne out. The direct consequence of this was that $\dot{m}$ could not be used as the independent variable in the display of thruster performance data, as is usually the case.

Annular Thruster

A schematic diagram of the thruster is shown in Fig. 1. The thruster body consists of two main parts, namely a core and a housing, each made of a martensitic stainless steel. A martensitic steel was used because of its hardness and small grain size which enable very sharp edges to be made. The core and housing are held together by a ring nut. The width of the annular slit, which exists between the sharp edges of the core and the housing depends upon the thickness of a phosphor-bronze spacer positioned between the two components. A neoprene O ring, slightly larger than the phosphor-bronze spacer prevents propellant leakage. Propellant from an annular reservoir flows along eight equi-spaced grooves in the core to an annular groove which is a few mm from the sharp edges of the thruster. All grooves are 0.5 mm deep and 0.5 mm wide.

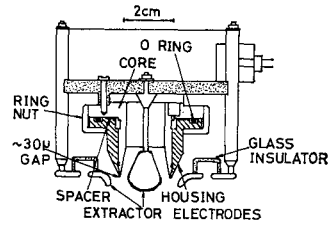

Fig. 1 Schematic diagram of the thruster.

The extractor electrodes are made of aluminum and are highly polished. The electrodes are insulated from each other and from Earth such that complete freedom of choice exists with respect to electrode potentials. The whole thruster assembly is housed in a screened cage to minimize electrostatic forces between the thruster and its environment.

Thruster Preparation

In order to ensure stable thruster operation, great care must be exercized during the preparation of the thruster for a test. The condition of the thruster edges is especially important. After normal machining of the edges, it was necessary to highly polish them using a lathe and the finest polishing paper available, with the thruster housing and core assembled together. Using this technique, sharp edges were produced which appeared, under microscopic examination from above, to have a thickness of less than 5 μ.

Various methods of measuring the profile of the emitter edges were investigated. One of the simplest of these was an imprinting technique using the metal indium, which is very soft at room temperature. A typical imprint of the annular thruster edges, as seen microscopically, is shown in Fig. 2. The edge height difference was due to the phosphor-bronze spacer, which is referred to in the previous section. In order to obtain some idea of the resolution of the imprinting technique, a razor blade impression was examined at a magnification of $\times 2000$. The edge thickness of the razor blade was known to be a small fraction of a micron and this was corroborated by the imprint. The imprinting technique was useful in giving an indication of edge sharpness, but each imprint is

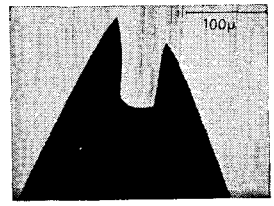

Fig. 2 Imprint in indium of thruster edges.

Received October 26, 1971; revision received February 22, 1972.
Index category: Electric and Advanced Space Propulsion.

* Visiting Scientist from The Electronics Department, Southampton University, England.
† Engineer.
‡ Member of Technical Staff.

only informative about one particular position on the edge. It was observed that if an edge was extremely clean, i.e. before a test, it was possible for the indium to cold-weld to it and thus damage it. For this reason, it was usual practice to postpone any imprinting until after the thruster had been run.

To ensure that the glycerol/sodium iodide propellant properly wets the thruster capillaries and edges, the thruster components must be scrupulously clean. One of the most effective cleaning methods we have found consists of an electrochemical treatment of the thruster core and housing using a strong solution of phosphoric acid. Each part of the thruster was connected to the positive side of a suitable power supply, immersed in the acid solution opposite a negative tungsten electrode and a current of about 5 amp was then passed through the circuit for ten seconds.

Test Facility

All thruster measurements were performed using a horizontal torsion balance[1] which was housed in a cylindrical stainless steel vacuum chamber of inside diameter 0.8 m and inside length 1.3 m. The chamber could be baked at about 100°C and then pumped down to about 10^{-7} torr when a liquid nitrogen cold trap was used. Without cooling, an ultimate pressure of about 10^{-6} torr was attainable. A diagram of the torsion balance showing also the annular thruster and the electrode configuration, which was used to suppress secondary effects, is shown in Fig. 3. The microbalance was sufficiently sensitive to resolve thrusts down to $10^{-7}N$. Its deflection and rate of change of deflection, which were proportional to thrust and propellant mass-flow rate respectively, were recorded on a chart recorder. Microbalance beam position was sensed by means of a differential capacitor arrangement which is fully described elsewhere.[1]

A sodium iodide/glycerol (20% NaI by weight) solution was used as the propellant in all tests. No elaborate procedures were adopted in the preparation of the propellant and it is possible that traces of water were present. NaI was added to pure glycerol, which was then heated to about 60°C in air. As soon as the salt had dissolved, the solution was placed under vacuum and was subsequently only exposed to air for a few minutes during transfer to the main propellant reservoir in the test facility. Outgassing problems did not arise.

The thruster reservoir was filled with propellant with the thruster in situ on the balance and under a vacuum of about 10^{-6} torr. The drip-feed system which was used for filling is shown in Fig. 3. Filling rate was controlled from outside the vacuum chamber via a pressure connection to the main propellant reservoir.

Experimental Procedure

Stable operation of the thruster was possible with the thruster maintained at either a positive or negative potential with respect to earthed accelerator electrodes. However, glow-discharge and breakdown problems occurred unless steps were taken to suppress secondary emission and backscatter from the collector. The arrangement depicted in Fig. 3 was satisfactory although the screen potential was fairly critical. For positive droplet spraying, the screen potential was maintained constant at -2kV. Glow-discharge and/or breakdown problems in the vicinity of the thruster edges arose if the screen potential was either a few hundred volts above or below -2kV. Similarly for negative spraying, the screen potential had to be about $+2$kV for stable thruster operation. It was not understood why the value of the screen potential was so critical. It was found necessary to include a series resistor with a resistance of several $M\Omega$ in the emitter supply line to stabilise thruster operation. The cooled honeycomb collector was definitely superior to a plane-surface collector with regard to the suppression of glow-discharges in the thruster region. Glow-discharges were assumed to be suppressed if there was no visible glow at the thruster rim when the vacuum chamber was completely dark.

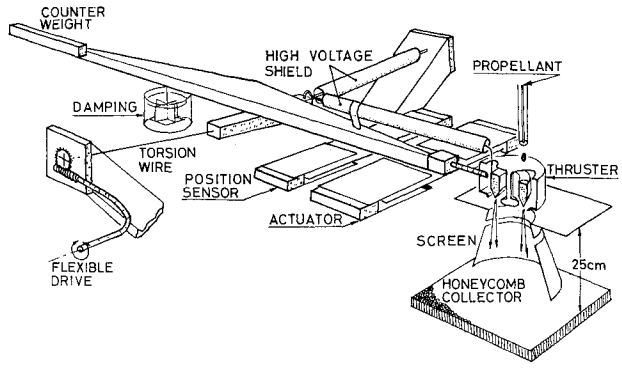

Fig. 3 Schematic diagram of the torsion balance.

Thruster voltage-current characteristics were first measured for both positive and negative spraying conditions. Thruster power supply voltage was increased in small steps from zero to a suitable maximum value and at each step, the current was noted alternately for positive and negative thruster potentials. From the measured current values, the voltage drop across the series stabilizing resistor was calculated and hence the thruster voltage with respect to Earth was determined.

Results

Thruster Voltage-Current Characteristics

The thruster voltage-current characteristics for positive and negative voltage spraying were almost identical. A typical characteristic is shown in Fig. 4. A 14 $M\Omega$ series resistor was present in the high-tension supply line to ensure stability of operation. At the highest current levels, i.e., above 350 μa breakdown problems in the vicinity of the thruster arose under negative voltage spraying conditions.

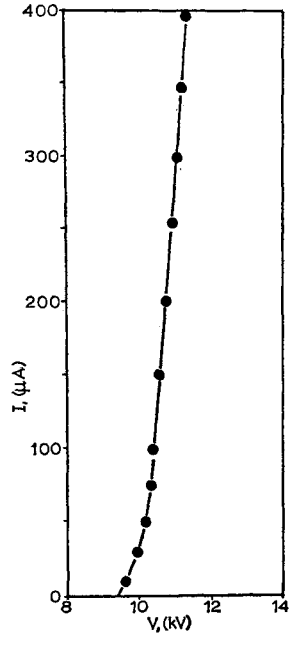

Fig. 4 Thruster voltage—current characteristic.

Thrust and Propellant Mass-Flow Rate

Two sets of typical thrust and mass-flow rate data were recorded from two experimental runs which were found to have different mass-flow rates, $\dot{m}$. Because of the extreme sensitivity to temperature of the propellant viscosity, a change in temperature resulted in a change in $\dot{m}$. The two sets of data were obtained on separate days when the mean ambient temperature differed by 5°C. Unfortunately, the temperature of the propellant within the thruster could not be monitored, but it was assumed that it did not differ greatly from the ambient temperature. The same phosphor-bronze spacer was used in all tests.

Mean Exhaust Velocity, Specific Charge and Thruster Efficiency

Thrust T is related to mass-flow rate $\dot{m}$ as follows:

$$T = \dot{m}\langle v \rangle \tag{1}$$

where $\langle v \rangle$ is the mean velocity of the exhaust in the direction of the thruster axis. $\langle v \rangle$ was determined from the measured values of T and $\dot{m}$.

Assuming that $\dot{m}$ was constant during each test run, it follows that the mean charge-to-mass ratio $\langle q/m \rangle$ of the exhausted propellant droplets must be a linear function of I because

$$\langle q/m \rangle = I/\dot{m} \tag{2}$$

This relationship and other performance data is shown graphically in Fig. 5.

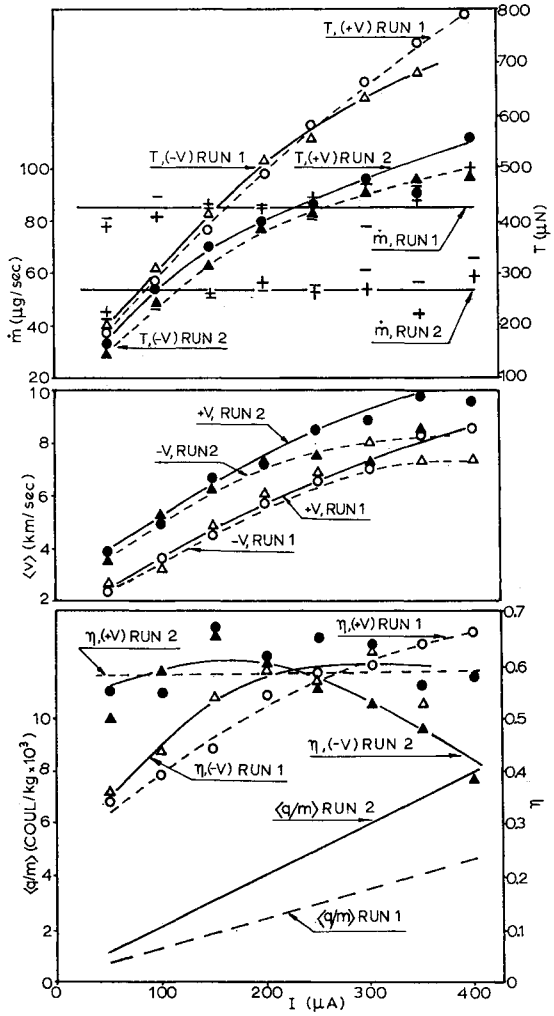

Fig. 5 Performance dependence on thruster current.

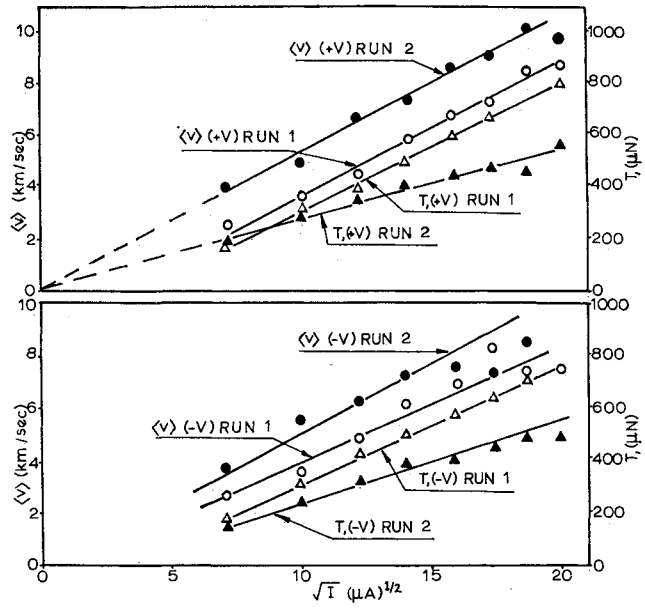

Fig. 6 Performance variation with the square root of current.

The efficiency of the thruster was calculated from the relation

$$\text{Efficiency} \quad \eta = T^2/2\dot{m}VI$$

where V is the voltage drop across the thruster alone. (Excluding the drop across the series resistor.) The graphs shown in Fig. 6 show thruster performance variation with the square root of thruster current.

Discussion of Results

Thruster characteristics obtained during positive voltage operation were similar in form to those obtained during negative voltage thrusting. Any differences that did occur were at the highest operating levels when breakdown problems occasionally arose during negative operation. For example, the thrust data for Run 2 shown in Fig. 6 shows a slight dropoff at current levels above 300 μa. It seems likely that hydrogen was liberated during negative operation and lead directly to breakdowns.

Over a current range of 25–400 μa, the voltage across the thruster changes by about 1.5 kv. This is only 15% of the total voltage across the thruster. If it is assumed that the electric field in the thruster emitting region is a linear function of applied voltage, it follows that thruster current must be a strong function of electric field in the emitting region.

It is believed that thruster current originates at a number of individual spraying sites which are distributed around the thruster rim. An increase of electric field at the rim causes an increase in the number of sites, the rate of increase determining the slope of the V/I characteristic. The rate at which the site density increases with voltage is directly related to rim geometry—particularly rim uniformity. We believe that a high degree of uniformity was achieved due to the extremely sharp edges of our thruster and that this was responsible for the observed steep V/I characteristic.

Due to the extreme sensitivity of the thruster to small changes in applied voltage, we chose to use thruster current as the 'independent' variable in the display of the operating characteristics.

Mass-Flow Rate

The mass-flow rate $\dot{m}$ during each experimental run was reasonably constant, particularly over the mid-region of the

current range. This differs from the data reported by Yahiku[2] et al. which showed that mass-flow rate was a linear function of thruster voltage, at constant feed pressure. However, it should be noted that their mass-flow rates were considerably lower than those considered here. Yahiku et al. stated that as a consequence of their linear relationship, specific impulse could not be increased by increasing thruster voltage. This was contrary to many of their other tests. It is noteworthy that even if $\dot{m}$ is voltage dependent, there is not likely to be much change in $\dot{m}$ over the operating range of the thruster reported here due to the near constancy of V. In any case, a constant $\dot{m}$ would not be unreasonable under some circumstances. In a capillary fed system, for example, there may be an upper limit to $\dot{m}$ which would occur when propellant is removed from the thruster edge region by electric forces as soon as it arrives. The edge region would thus be virtually propellant free except for a thin surface film. Only under very low voltage operation, or with no voltage applied to the thruster, would a relatively large volume of propellant occupy the edge region.

The data of Yahiku et al. demonstrates the extreme sensitivity to temperature of mass-flow rate due to propellant viscosity changes. The data shown in Fig. 5 suggest that temperature was fairly constant during each experimental run. The observed 5°C temperature change in the laboratory was sufficient to account for the difference in mass-flow rates between the two runs.

Thruster Efficiency

Thruster exhaust velocity, $\langle v \rangle$, is related to the thruster accelerating voltage V by:

$$\langle v \rangle \alpha [2\langle q/m \rangle V]^{1/2} \tag{3}$$

However, as is shown in Fig. 4, V only changes by 15% over the entire thruster range of operation. If it is assumed that V is constant, it follows that

$$\langle v \rangle \propto \langle q/m \rangle^{1/2} \tag{4}$$

and from Eqs. (1) and (2) we have

$$\langle v \rangle \propto I^{1/2},\ T \propto I^{1/2} \tag{5}$$

The experimental data plotted in Fig. 6 verify Eqs. (5). The thrust data may be represented as

$$T = -a + bI^{1/2} \tag{6}$$

where a and b are constants found from the graphs shown in Fig. 6.

The efficiency of the thruster η is given by the expression

$$\eta = T^2/2\dot{m}VI = a^2/2\dot{m}VI - ab/\dot{m}VI^{1/2} + b^2/2\dot{m}V \tag{7}$$

By differentiation

$$d\eta/dI = -a^2/2\dot{m}VI^2 + ab/2\dot{m}VI^{3/2} \tag{8}$$

This expression is zero when

$$a/I^2 = b/I^{3/2}$$

i.e., when

$$I^{1/2} = a/b \tag{9}$$

This point is the abscissa intercept on the $T/I^{1/2}$ graph and it is obvious that at this point, the thruster efficiency is zero. At current levels below the intercept, although the efficiency is positive, it is clearly meaningless. However, for currents above the intercept, in the thruster operating range, the efficiency is given by Eq. (7). This expression indicates a rising η as I increases until at large values of I, the first two terms become negligible in comparison with the final term such that

$$\eta \to b^2/2\dot{m}V \tag{10}$$

It is interesting to note that if the $T/I^{1/2}$ curve can be extrapolated back through the origin such that the const $a = 0$, then η is given by Eq. (10) and is independent of thruster current. This effect may be demonstrated by considering the positive-voltage data from Run 2. Reference to Fig. 6 shows that the T curve may be extrapolated back through the origin. The T relationship is given by

$$T = 2.6.\ \ 10^{-2} I^{1/2}$$

i.e. $b = 2.6.\ 10^{-2}\ N/(\text{amp})^{1/2}$. If the average $\dot{m}$ value for Run 2 is taken ($5.4\ 10^{-8}$ kg/sec) and V *is* assumed to be 10.8 kv, then expression (10) gives $\eta = 0.58$ which is in accord with the data shown in Fig. 5.

The stabilisor resistor in the thruster voltage-supply line caused a reduction in over-all efficiency which has not been accounted for in the efficiency calculations. However, the instability was thought to be due to a deficiency in the power supply unit. With a properly stabilized supply, the thruster would almost certainly be stable in operation such that over-all efficiency would not be reduced.

If during normal thruster operation, most of the applied voltage is used to accelerate droplets, then the mean velocity $\langle v \rangle$ of the droplets is given by

$$\langle v \rangle \approx (2IV/\dot{m})^{1/2} \tag{11}$$

Assuming there is no beam divergence, it follows that

$$T = \dot{m}\langle v \rangle \approx (2\dot{m}V)^{1/2} I^{1/2} \tag{12}$$

By comparing Eqs. (6) and (12), it follows that

$$b \approx (2\dot{m}V)^{1/2} \tag{13}$$

The slopes of the $T/I^{1/2}$ curves are in reasonable agreement with this expression. The thruster running voltage V will be dependent upon geometry, particularly the sharpness of the emitter edges. It seems reasonable to assume that the sharper are the edges, the lower will be V. The implication of Eq. (13) however, is that for any particular geometry and hence value of V, the mass-flow rate can be controlled to adjust the slope of the $T/I^{1/2}$ characteristic. A particular value of $\dot{m}$ might permit the characteristic to be extrapolated back through the origin such that thruster efficiency would be constant over the operating range.

Conclusions

The operating characteristics of a capillary-fed annular thruster are considered. There is little difference between positive voltage and negative voltage thrusting. The thruster voltage-current characteristic resembles that of a zener diode and it is possible to assume that the thruster voltage is constant over a thruster current range of 50–400 μa. Propellant mass-flow rate is also fairly constant over the operating range. It follows that thrust and exhaust velocity are linear functions of the square root of thruster current. Under certain conditions, it is possible for thruster efficiency to be constant over a considerable current range of operation.

References

[1] Bailey, A. G., Bracher, J. E., Helmke, H. G., and von Rohden, H. J., "A Test Facility for Electric Microthrusters," *Review of Scientific Instruments*, Vol. 43, No. 3, March 1972, pp. 420–424.

[2] Yahiku, A. Y., Mahoney, J. F., Daley, H. L., Perel, J., and Sharman, A., "Experimental Study of Colloid Annular Thrusters," AIAA Paper 70-1112. Stanford, Calif., 1970.